

Electronic band structure of HgSe from Fourier transform spectroscopy

M. von Truchseß, A. Pfeuffer-Jeschke, C. R. Becker, G. Landwehr, and E. Batke

Physikalisches Institut der Universität Würzburg, Am Hubland, D-97074 Würzburg, Federal Republic of Germany

(Received 6 October 1999)

Magneto-optical investigations were performed at liquid helium temperatures with Fourier transform spectroscopy to clarify the electronic band structure of HgSe. Two characteristic sets of interband transitions were observed that allow us to determine the band structure without the necessity of referring to a theoretical model. Our experiment demonstrates unambiguously that HgSe is a semimetal with inverted-type electronic-band structure and not a semiconductor, as was recently deduced from photoemission spectroscopy.

In a recent paper Gawlik *et al.*¹ concluded from photoemission spectroscopy that HgSe, a prototype material of the group of mercury rich II-VI compounds, is a semiconductor with a positive fundamental gap of 420 meV at 300 K. More recently a value of 330 meV was determined at 30 K.² This is in total disagreement with previous magnetotransport,³ optical,^{4,5} and magneto-optical⁶ experiments that were interpreted in terms of an inverted-type electronic band structure characteristic for a semimetal. A clarification of this controversy is of fundamental importance. Unfortunately, *ab initio* calculations of the band structure cannot solve the problem. Depending on the theoretical approach either the band structure of a semiconductor or a semimetal is obtained.⁷ Therefore an unambiguous experimental verification of the band structure is required. Conclusions derived from previous transport and spectroscopic investigations rely on a comparison to $\mathbf{k}\cdot\mathbf{p}$ band-structure calculations, which one might criticize as a weakness of those attempts. Consequently, an approach based on qualitative considerations that allows the band structure to be determined without the necessity of referring to a specific numerical calculation is preferable. This can be done with a magneto-optical investigation which cov-

ers sufficiently wide frequency and magnetic-field ranges, as we demonstrate in the following.

Our samples were 1- μm -thick *n*-type HgSe epitaxial layers grown by molecular-beam epitaxy on (100) GaAs substrates. Due to the large lattice mismatch between HgSe and GaAs, a 5- μm ZnTe buffer was deposited first to improve the structural quality. The growth was performed at temperatures of 325 and 105 °C for the ZnTe and HgSe layers, respectively. All previously known HgSe samples were *n*-type and had electron concentrations on the order of 10^{17} or 10^{18} cm^{-3} . In order to reduce the free-electron concentration in our samples we intentionally counterdoped the epitaxial layers with As. Due to compensation these epitaxial layers have an exceptionally low electron concentration of less than $3 \times 10^{16}\text{ cm}^{-3}$ at 5 K as deduced from the Fermi energy and confirmed via electron cyclotron resonance data. Information on the band structure was gathered via the normalized transmission $T(B)/T(0)$ for unpolarized radiation which was incident parallel to a magnetic field B oriented in the growth direction.

In Fig. 1 the normalized transmission $T(B)/T(0)$ is shown for the frequency regimes (a) 40–260, (b) 400–4000,

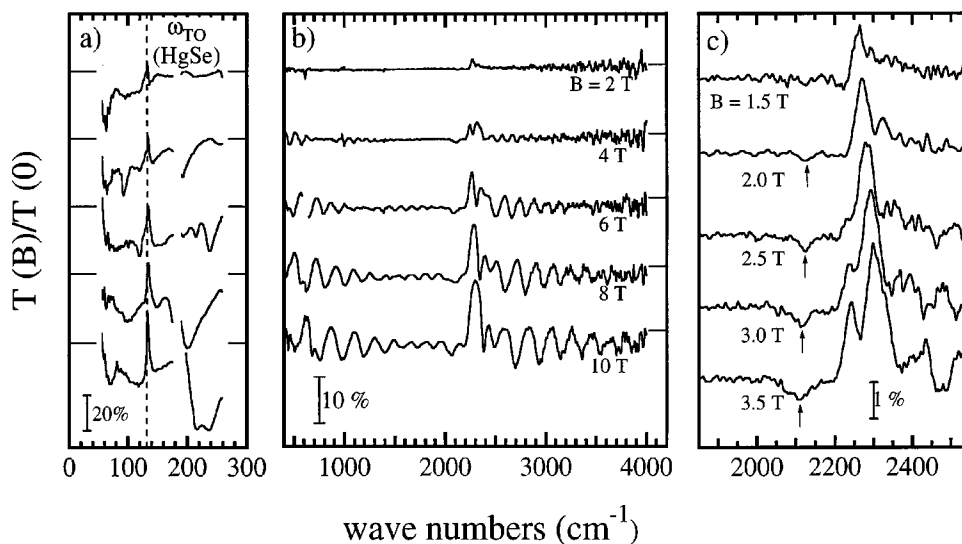


FIG. 1. Normalized magnetic-field-dependent transmission $T(B)/T(0)$ for a HgSe epitaxial layer at 5 K in frequency regimes (a) 40–260 cm^{-1} , (b) 400–4000 cm^{-1} , and (c) 1850–2550 cm^{-1} . The horizontal bars indicate $T(B)/T(0)=1$ baselines. In (a) the dashed vertical line indicates the position of the transverse optical phonon of HgSe, and in (c) arrows mark the positions of a transition with negative magnetic-field dispersion.

and (c) $1850\text{--}2550\text{ cm}^{-1}$. The frequency regimes from about 180 to 200 and 260 to 350 cm^{-1} are opaque due to strong reststrahlen absorption of ZnTe and GaAs, respectively. All resonant structures shown in Figs. 1(b) and 1(c) represent interband transitions. We arrive at this conclusion from a consideration of the resonance line shapes. In a strong magnetic field, transitions can only occur between Landau bands, resulting from a quantized carrier motion perpendicular to the magnetic-field direction and an unconstrained motion parallel to it. In the case of a nonparabolic system, whose initial and final Landau bands have opposite curvatures, the interband separations increase with increasing wave vector parallel to the magnetic-field direction. Under these circumstances one expects asymmetric resonance line shapes for interband transitions exhibiting high frequency tails.⁸ With one exception the resonances shown in Figs. 1(b) and 1(c) have this line shape. The asymmetry can very clearly be recognized on an enlarged scale.

As is obvious from Fig. 1(b) there are two sets of interband transitions, one dominates below and the other above about 2250 cm^{-1} . A closer look at the higher energy set in the lower magnetic-field range is given in Fig. 1(c). The maxima appearing at about 2250 cm^{-1} in the normalized spectra $T(B)/T(0)$ reflects the onset of the interband transition at zero magnetic-field strength, whereas the minima appearing above 2250 cm^{-1} represent interband transitions between Landau bands at finite magnetic-field strengths B . This we conclude following the line-shape argument discussed above. In addition, an essentially symmetric resonance whose position is marked by an arrow, is observed at about 2100 cm^{-1} . At sufficiently small magnetic-field strengths this resonance decreases in energy with increasing magnetic-field strength. This is in contrast to all other resonances of this set that exhibit a positive magnetic-field dispersion and asymmetric line shapes. Upon extrapolating the resonances to the limit of vanishing magnetic field, both the resonance with a negative and the remainder with a positive dispersion give essentially the same energy value. Thus, we conclude that the unusual resonance is also an interband transition. The simultaneous observation of interband transitions with positive and negative magnetic-field dispersion which extrapolate to a finite energy in the limit of vanishing B , allows the following conclusions: (1) the initial and the final bands are separated by an energy of approximately 277 meV, (2) the curvature of the initial and the final bands have the same sign at the Brillouin-zone center with the effective mass of the initial state being smaller than that of the final state, and (3) there has to be a reversal in sign for the curvature of the initial band at some finite wave vector. On the other hand, the interband transitions of the low-energy set as shown in Fig. 1(b) below about 2100 cm^{-1} all have a positive magnetic-field dispersion and extrapolate essentially to zero energy in the limit of vanishing B . Thus, we conclude that (1) the initial and final bands are degenerate at the Brillouin zone center, and (2) the initial and final bands have opposite curvatures.

In Fig. 2 the resonance positions of the two interband transitions are shown in a magnetic-field regime up to 12 T. We recorded spectra at 250 different magnetic-field strengths in this regime, providing more than 4000 data points. The resonance near 2100 cm^{-1} with negative magnetic-field dis-

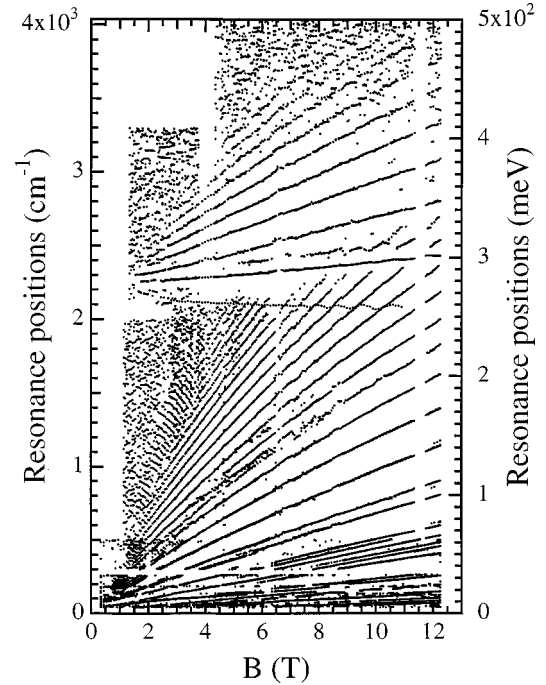


FIG. 2. Interband transition energies versus magnetic field strength for a HgSe epitaxial layer at 5 K.

person can clearly be recognized. We could trace the resonance positions down to about 1 T, which indicates that the Burstein-Moss^{9,10} shift in our samples is very small. This is important for the observation of the interband transition which exhibits a negative magnetic field dispersion at sufficiently small magnetic-field strengths. Presumably, this unusual resonance has not been observed previously due to the larger electron concentrations and the consequently enhanced Burstein-Moss shift in prior investigations. We also note that the interband transition extrapolating to zero energy in the limit of vanishing magnetic-field strength was not observed before.

With all this information now available it is possible to distinguish between the band structures of a semiconductor and a semimetal. For qualitative considerations we calculated the bulk band structures in the framework of the quasigermanium model¹¹ for a semiconductor and a semimetal as shown, respectively, in Figs. 3(a) and 3(b). The calculation was performed with band parameters as given in Ref. 4 for HgSe. In Fig. 3(a) we assumed that the fundamental band gap $E_g = E_{\Gamma_6} - E_{\Gamma_8} = 330\text{ meV}$ as deduced from photoemission² at 30 K, whereas in Fig. 3(b) we assumed $E_g = -268\text{ meV}$ as deduced previously from magneto-absorption⁶ at 10 K. In case of a semiconductor the conduction band is an s -like band of Γ_6 symmetry, and the p -like bands of Γ_8 and Γ_7 symmetry constitute the valence bands. At the center of the Brillouin zone the heavy- and light-hole Γ_8 bands are degenerate and the Γ_7 band is separated by the spin-orbit split-off energy Δ_0 from the valence-band edge. For a semimetal the band structure is inverted, i.e., compared to a semiconductor the relative positions of the bands with Γ_6 and Γ_8 symmetry are reversed. This situation is formally expressed by a negative value of the fundamental gap $E_g = E_{\Gamma_6} - E_{\Gamma_8}$. Our sample is n -type and the Fermi energy, which is on the order of a couple of meV, has to be either in

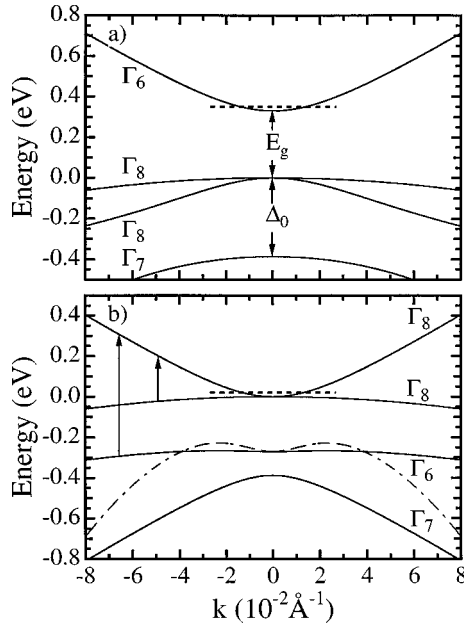


FIG. 3. Calculated electronic band structure for (a) a semiconductor and (b) a semimetal within the quasigermanium model. In (a) a fundamental gap of 330 meV and in (b) -268 meV is assumed. The dashed horizontal lines indicate the Fermi energy. The dash-dotted line in (b) shows the dispersion of the valence band with Γ_6 symmetry on an energy scale which is magnified by a factor of 10.

the Γ_6 band (semiconductor) or in the Γ_8 band (semimetal). Considering the fact that an interband transition occurs between bands that are degenerate at the Brillouin-zone center, it is evident that the band structure of a semiconductor is inconsistent with the experimental results. Only the inverted band structure agrees with experiment. The observed $\Gamma_8 \rightarrow \Gamma_8$ and $\Gamma_6 \rightarrow \Gamma_8$ interband transitions are indicated by arrows in Fig. 3(b). Please note the camelback type dispersion of the Γ_6 band in Fig. 3(b). For clarity the dispersion of the Γ_6 band at the zone center has also been magnified by a factor of ten as shown with a dash-dotted line. There is a sign reversal of the band curvature at finite wave vector. This is the feature necessary to explain the observed interband transition with negative magnetic-field dispersion.

A quantitative analysis of our experiment (Fig. 2) within the framework of the quasigermanium model is shown in Fig. 4. The best overall agreement with the experiment is obtained with the band parameters $E_p = 15.2$ eV, $\Delta_0 = 387$ meV, $\gamma_1 = 2.0$, $\gamma_2 = -0.25$, $\gamma_3 = 0.42$, $\kappa = -0.58$, and $F = N_1 = 0$. Our calculation includes strain in the HgSe epitaxial layer. The influence of strain is evident in the experimental transition energies in the zero-field limit. The $\Gamma_6 \rightarrow \Gamma_8$ transitions extrapolate to a value of about 277 meV, which is somewhat higher than the fundamental gap deduced previously for bulk samples. In addition, the $\Gamma_8 \rightarrow \Gamma_8$ transitions do not all extrapolate to zero energy in the limit of vanishing B . Several transitions extrapolate to a small finite energy of about 4 meV. At liquid nitrogen temperatures the lattice constant of the ZnTe buffer layer is somewhat smaller than that of bulk HgSe. This results in a biaxial compression of the HgSe lattice with an additional elongation of the lattice in the growth direction. It is well known that this results

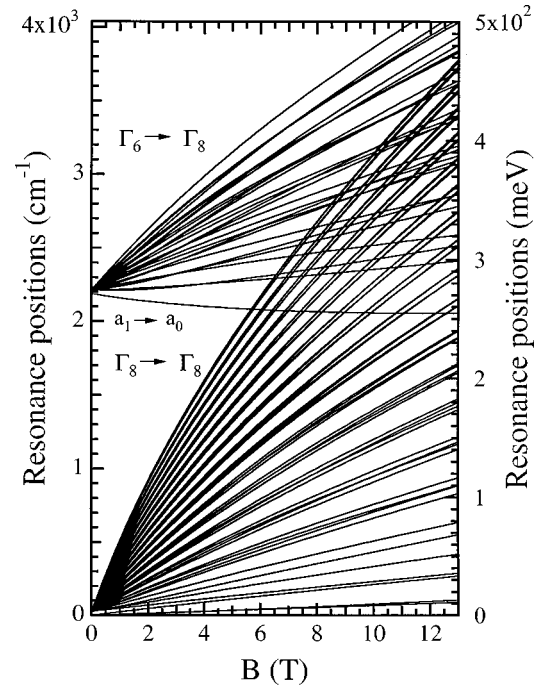


FIG. 4. Predicted resonance positions for the experiment shown in Fig. 2. The calculation was performed within the framework of the quasigermanium model including strain in the HgSe epitaxial layer. The transition with negative magnetic-field dispersion is a $a_1 \rightarrow a_0$ transition between the bands of Γ_6 and Γ_8 symmetry in the notation of Weiler (Ref. 11).

in an enlargement of the Γ_6 - Γ_8 band gap and a lifting of the degeneracy of the Γ_8 bands at the Brillouin-zone center.¹² Our calculation in Fig. 4 assumes a splitting energy of 4 meV at liquid helium temperatures. From the calculation we obtain a value of -272 meV at 5 K, which includes the fundamental bulk gap and a small shift on the order of -2 meV arising from the hydrostatic component of the strain. Note that our fundamental gap of -274 meV is in very good agreement with the bulk value of -272 meV given in Ref. 6 for 5 K. The uncertainty due to strain is very small and without consequences to the question of whether HgSe is a semiconductor or a semimetal.

There has been a theoretical prediction that in the inverted case the sequence of the bands might be Γ_8 - Γ_7 - Γ_6 instead of Γ_8 - Γ_6 - Γ_7 as is shown in Fig. 3(b).¹³ This seems unlikely considering the fact that our experiment is correctly explained assuming a Γ_8 - Γ_6 - Γ_7 sequence. Exchanging the values of Δ_0 and E_g but keeping the above values for the other band parameters, the experiment cannot be explained assuming a Γ_8 - Γ_7 - Γ_6 sequence. Such a sequence seems also unlikely in the context of a qualitative consideration of the oscillator strengths. Transitions between the p -like bands, $\Gamma_8 \rightarrow \Gamma_8$ and $\Gamma_7 \rightarrow \Gamma_8$ are symmetry forbidden at the center of the Brillouin zone. Only for a finite wave vector or finite magnetic-field strength where band mixing occurs, are the electric dipole matrix elements (M_E) finite. The $\Gamma_8 \rightarrow \Gamma_8$ transitions owe their strength to the fact that the transition frequencies ω are comparatively small, which boosts their oscillator strength proportionally according to $|M_E|^2/\omega$. This effect is negligible for $\Gamma_7 \rightarrow \Gamma_8$ transitions in the case of a large band separation. Thus, for the same band separation,

the $\Gamma_7 \rightarrow \Gamma_8$ transitions should have smaller oscillator strengths than the $\Gamma_6 \rightarrow \Gamma_8$ transitions. In view of the fact that the oscillator strength for the high-energy set is large, it seems unlikely that the band of Γ_7 symmetry is above the band of Γ_6 symmetry.

In conclusion, a magneto-optical investigation of n -type HgSe epitaxial layers over a wide range of frequencies and magnetic fields has revealed two characteristic sets of interband transitions that unambiguously define the qualitative electronic band structure. Without relying on a theoretical calculation we demonstrated that HgSe is a semimetal with

inverted-type band structure. At 5 K we obtained a fundamental bulk gap of -274 meV between the Γ_8 conduction band and the valence band with Γ_6 symmetry. We can exclude the possibility that HgSe is a semiconductor as was proposed from photoelectron spectroscopy.

We would like to gratefully acknowledge financial support by the Deutsche Forschungsgemeinschaft via SFB 410. We would also like to thank N. Orłowski, J. Pollmann, and A. Fleszar for valuable discussions and their permission to quote unpublished results.

¹K. U. Gawlik, L. Kipp, M. Skibowski, N. Orłowski, and R. Manke, Phys. Rev. Lett. **78**, 3165 (1997).

²Fundamental gap deduced from photoemission at 30 K, N. Orłowski (private communication).

³S. L. Lehoczky, J. G. Broerman, D. A. Nelson, and C. R. Whittsett, Phys. Rev. B **9**, 1598 (1974).

⁴W. Szuskiewicz, Phys. Status Solidi B **91**, 361 (1979).

⁵S. Einfeldt, F. Goschenhofer, C. R. Becker, and G. Landwehr, Phys. Rev. B **51**, 4915 (1995).

⁶M. Dobrowolska, W. Dobrowolski, and A. Mycielski, Solid State Commun. **34**, 441 (1980).

⁷J. Pollmann (private communication); A. Fleszar (private communication).

⁸B. König, A. Pfeuffer-Jeschke, S. Oehling, C. R. Becker, and E.

Batke, in *Proceedings of the 12th International Conference on High Magnetic Fields in Semiconductors*, edited by G. Landwehr and W. Ossau (World Scientific, Singapore, 1996), pp. 821–824.

⁹E. Burstein, Phys. Rev. **93**, 632 (1954).

¹⁰T. S. Moss, Proc. Phys. Soc. London, Sect. B **76**, 775 (1954).

¹¹M. H. Weiler, in *Defects, (HgCd)Se, (HgCd)Te*, Semiconductors and Semimetals Vol. 16, edited by R. K. Willardson and A. C. Beer (Academic, New York, 1981), p. 119.

¹²F. H. Pollak, in *Strained-Layer Superlattices: Physics*, Semiconductors and Semimetals Vol. 32, edited by R. K. Willardson and A. C. Beer (Academic, New York, 1990), p. 17.

¹³M. Rohlffing and S. G. Louie, Phys. Rev. B **57**, 9392 (1998).